Synthesis, X-ray Powder Structure, and Magnetic Properties of Layered Ni^{II} Methylphosphonate, $[Ni(CH_3PO_3)(H_2O)]$, and Ni^{II} Octadecylphosphonate, $[Ni\{CH_3\text{-}(CH_2)_{17}\text{-}PO_3\}(H_2O)]$

Carlo Bellitto,*[a] Elvira M. Bauer,[a] Said A. Ibrahim,[b] Mohamed R. Mahmoud,[b] and Guido Righini[a]

Abstract: $[Ni(CH_3PO_3)(H_2O)]$ (**1**) and $[Ni\{CH_3\text{-}(CH_2)_{17}\text{-}PO_3\}(H_2O)]$ (**2**) were synthesised by reaction of $NiCl_2 \cdot 6H_2O$ and the relevant phosphonic acid in water in presence of urea. The compounds were characterised by elemental and thermogravimetric analyses, UV-visible and IR spectroscopy, and their magnetic properties were studied by using a SQUID magnetometer. The crystal structure of **1** was determined "ab initio" from X-ray powder diffraction data and refined by the Rietveld method. The crystals of **1** are orthorhombic, space group $Pmn2_1$, with $a = 5.587(1)$, $b = 8.698(1)$, $c = 4.731(1)$ Å. The compound has a hybrid, layered structure made up of alternating inorganic and organic layers along the b direction of the unit-cell. The inorganic layers consist of Ni^{II} ions octahedrally coordinated by five phosphonate oxygen atoms and one oxygen atom from the water molecule. These layers are separated by bilayers of methyl groups and van der Waals contacts are established between them. A preliminary structure characterisation of compound **2** suggests the crystallisation in the orthorhombic system with the following unit-cell parameters: $a = 5.478(7)$, $b = 42.31(4)$, $c = 4.725(3)$ Å. The oxidation state of the Ni ion in both compounds is +2, and the electronic configuration is d^8 ($S = 1$), as determined from static magnetic susceptibility measurements above 50 K. Compound **1** obeys the Curie–Weiss law at temperatures above 50 K; the Curie (C) and Weiss (θ) constants were found to be 1.15 $cm^3 K mol^{-1}$ and −32 K, respectively. The negative value of θ indicates an antiferromagnetic exchange coupling between near-neighbouring Ni^{II} ions. No sign of 3D antiferromagnetic long-range order is observed down to $T = 5$ K, the lowest measured temperature. Compound **2** is paramagnetic above $T = 50$ K, and the values of C and θ were found to be 1.25 $cm^3 K mol^{-1}$ and −24 K, respectively. Below 50 K the magnetic behavior of **2** is different from that of **1**. Zero-field cooled (zfc) and field-cooled (fc) magnetisation plots do not overlap below $T = 21$ K. The irreversible magnetisation, ΔM_{fc-zfc}, obtained as a difference from fc and zfc plots starts to increase at $T = 20$ K, on lowering the temperature, and it becomes steady at $T = 5$ K. The presence of spontaneous magnetisation below $T = 20$ K indicates a transition to a weak-ferromagnetic state for compound **2**.

Keywords: layered compounds · magnetic properties · nickel · phosphonates · structure elucidation.

Introduction

Metal(II) phosphonates, $[M(RPO_3)(H_2O)]$[1] and bisphosphonates, $[M_2(O_3P\text{-}R\text{-}PO_3)(H_2O)_2]$[2] (in which M is a divalent metal ion, and R is an alkyl or aryl group) represent an interesting class of layered metal–salt compounds.[3–4] $[M^{II}(R\text{-}PO_3)(H_2O)]$ (M = Cd, Mn, Fe, Co, Ni, Zn) crystallise mainly in layered structures composed of metal ions and the phosphonate oxygen atoms lying in puckered sheets. The pendent organic R group occupies the interlamellar space, and two organic layers with van der Waal contacts are interspersed with the inorganic ones. The number of carbon atoms in the organic chain can be varied and the interlamellar distance can be then increased. It has been shown that the structures of divalent metal phosphonates tend to comprise zigzag layers with the metal ion six-coordinate (see Figure 1).[5–7]

For each phosphonate group two oxygens form a bridge between a pair of metal atoms, whereas the third oxygen is coordinated to only one metal atom. Each metal atom is thus

[a] Dr. C. Bellitto, Dr. E. M. Bauer, Dr. G. Righini
CNR-Istituto di Struttura della Materia, Sez.2
Via Salaria Km. 29.5, C.P.10
00016 Monterotondo Stazione, Roma (Italy)
Fax: (+39) 06-9067-2316
E-mail: carlo.bellitto@ism.cnr.it

[b] Prof. Dr. S. A. Ibrahim, Prof. Dr. M. R. Mahmoud
Department of Chemistry, Faculty of Science
University of Assiut, Assiut (Egypt)

Supporting information for this article is available on the WWW under http://www.chemeuj.org or from the author. Table S1 provides a complete listing of atomic parameters and isotropic thermal displacement parameters for $[Ni(CH_3PO_3)(H_2O)]$.

0947-6539/03/0906-1324 $ 20.00+.50/0

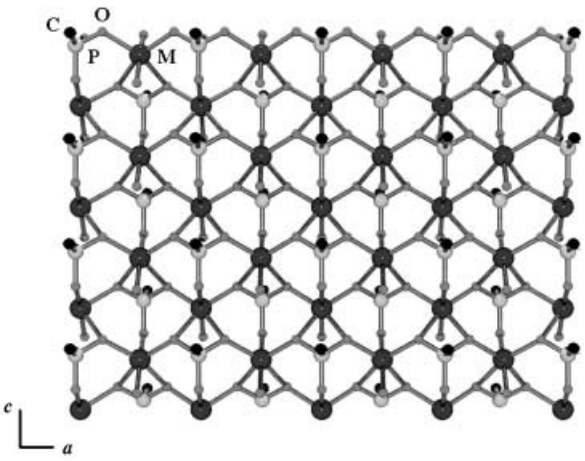

Figure 1. Zigzag-layered structure of divalent metal phosphonates.

surrounded by six oxygens in a distorted octahedral coordination. These six oxygens comprise four bridging, one terminal, and one from a water molecule. The resulting 2D lattice is interesting from the point of view of the search for new low-dimensional magnetic materials and for thin-film magnetic solids. The two-dimensional nature of the crystal lattice in paramagnetic metal(II) phosphonates favours the next-neighbour-exchange magnetic interaction and, at low temperatures, a long-range magnetic ordering is often observed.[8]

We have recently reported on several paramagnetic divalent metal phosphonates $[Cr(CH_3PO_3)(H_2O)]$,[9] $[Fe_2\{O_3P\text{-}(CH_2)_n\text{-}PO_3\}(H_2O)_2]$,[10] $[Fe(C_6H_5PO_3)(H_2O)]$[11] and $[Fe(CH_3\text{-}PO_3)(H_2O)]$,[12, 7] and we found that these compounds order antiferromagnetically at low temperatures. Below the antiferromagnetic-ordering temperature (T_N) the equilibrium distribution of the magnetic moment is not perfectly antiparallel, as would be expected for an antiferromagnet, but canted from the magnetic easy axis giving rise to a spontaneous magnetisation. This phenomenon is better known as "canted antiferromagnetism" or "weak-ferromagnetism" and it has been observed for the first time in α-Fe_2O_3.[13] For divalent transition metals, most studies were carried out within the field of inorganic solid-state chemistry and the main difficulty was the lack of a general procedure for the formation of the crystalline materials, possibly single crystals. For example, a recent report on nickel(II) methylene-*bis*-phosphonates by Cheetham et al. showed that a phosphonate Ni^{II} compound of formula $[Ni_4\{O_3P\text{-}(CH_2)\text{-}PO_3\}_2(H_2O)_3]$ could be prepared by using an hydrothermal method.[14] It dehydrates topotactically in two steps, giving firstly $[Ni_4\{O_3P\text{-}(CH_2)\text{-}PO_3\}_2(H_2O)]$ and then $[Ni_4\{O_3P\text{-}(CH_2)\text{-}PO_3\}_2]$. The crystal structures are different from those reported for other divalent transition metal ions. The first one is built from sheets of trimeric edge-sharing units of octahedral Ni^{II} ions, on which octahedral Ni and the diphosphonate groups are grafted. The second one, having lost a water molecule, has one Ni^{II} tetrahedrally coordinated and the structure is 3D. The anhydrous compound on the other hand contains Ni^{II} in six-, five- and fourfold coordination. More interesting the magnetic behaviour of these compounds is different. $[Ni_4\{O_3P\text{-}(CH_2)\text{-}PO_3\}_2(H_2O)_2]$ shows ferromagnetic interaction and a long-range ferromagnetic ordering at $T = 3.8$ K. Further, another recent report has appeared on similar nickel(II) organo-phosphonates. In this case the compounds were prepared by a solid-state reaction of a stoichiometric mixture of phosphonic acid and nickel(II) hydroxide at the melting point of the ligand, but no crystal structure and magnetic studies were reported.[15] We have found a general method of preparation of metal(II) phosphonates that provides at least a microcrystalline product, and has allowed us to grow single crystals in the case of $[Fe(CH_3PO_3)\text{-}(H_2O)]$.[7]

This paper deals with the synthesis and magnetic properties of $[Ni(CH_3PO_3)(H_2O)]$ (**1**) and of $[Ni\{CH_3\text{-}(CH_2)_{17}\text{-}PO_3\}\text{-}(H_2O)]$ (**2**) and the "ab initio" X-ray powder structure determination of **1**. The compounds were studied mainly for two reasons: 1) to study the influence of the organic thickness on their magnetic properties and 2) the synthesis of a truly 2D magnetic system.

Results and Discussion

Ni^{II} alkylphosphonates were prepared from the reaction of the relevant phosphonic acid in water, with $NiCl_2 \cdot 6H_2O$ in the presence of urea at temperatures above 80–90 °C. Under these conditions urea decomposes to give ammonium carbonate, thus rising gradually the pH of the solution. The compounds were precipitated as greenish-yellow microcrystalline powders after days of reflux. The final pH of the solution was found to be near the neutrality. This method has been proved to be general for the synthesis of several divalent metal phosphonates. Both compounds were characterised by elemental analyses, thermogravimetric analysis (TGA), differential scanning calorimetry (DSC) and X-ray powder diffraction (XRPD) techniques, as well as by the electronic and FT-IR absorption spectroscopy. The TGA of compound **1** shows stepwise mass losses. Below 100 °C < 1 % of loss is due to adsorbed water. The compound starts to lose coordinated water at 107 °C and it stops at ~280 °C. The observed weight loss at this stage is 10.21 %, a value which corresponds to one water molecule per formula unit (the calculated weight loss for one water molecule per formula unit is 10.54 %). The compound is then stable up to 570 °C, when it starts to decompose, loosing the organic part of the ligand. The TGA of compound **2** shows one mass loss between 50 to 100 °C (2.3 %) due to the water of crystallisation or adsorbed water. The compound then starts to lose coordinated water at ~130 °C and it stops at 270 °C. The observed weight loss at this stage is 5.2 %, a value that corresponds roughly to one water molecule per formula unit. The calculated weight loss for one water molecule is 4.40 %. Above 280 °C the compound starts to decompose and stops at 570 °C, loosing the 52.89 % of the weight, corresponding to the aliphatic chain of the ligand in the compound.

Crystal structure of $[Ni(CH_3PO_3)(H_2O)]$ (1): The X-ray powder diffraction spectra of **1** was recorded, and the crystal structure was solved "ab initio" and refined by the Rietveld method (see Experimental Section). The final R_p, R_{pw} and R_F

  0947-6539/03/0906-1325 $ 20.00+.50/0

agreement factors, together with details of data collections and analyses for the compound **1** are given in Table 1. The final Rietveld plots are shown in Figure 2. The lists of bond lengths and angles are reported in Table 2 and final fractional coordinates are reported in Table S1, supplied as Supporting Information.

Ni^{II} methylphosphonate crystallises in a lamellar structure and is isomorphous to several $[M^{II}(CH_3PO_3)(H_2O)]$ (M = Mg, Mn, Zn) complexes, the crystal structures of which have been previously reported.[6a] The unit-cell packing of compound **1** along the *c* axis is shown in Figure 3 and the projection along the *b* axis is presented in Figure 4. The Ni atom is six-coordinate, surrounded by five oxygens of the phosphonate groups (O2,O3) and one from the water molecule (O1). As the compound contains only one ligand per metal ion, all the phosphonate oxygen atoms take part in metal binding; two oxygens (O2) chelate the metal ions and at the same time bridge adjacent metal ions in the same row. Oxygen O3 of the phosphonate lying in the mirror plane bonds to only one Ni atom and is located *trans* to the oxygen of the water molecule (i.e., 168.6°). The octahedron is distorted and one of the lowest *cis* O-Ni-O angles is 64°, while the others range between 96 to 103.2°. The P–C bonds are inclined by ~7° with respect to the *b* axis. The layers are translationally related along the *b* axis. This kind of organic–inorganic layered structure has been observed previously in $[Cd(CH_3PO_3)(H_2O)]$,[5] and in $[Fe(CH_3PO_3)(H_2O)]$.[7, 12]

Table 1. Crystallographic data for $[Ni(CH_3PO_3)(H_2O)]$ (**1**).

formula	NiO_4PCH_5
M_r	170.72
space group	$Pmn2_1$ (no. 31)
a [Å]	5.587 (1)
b [Å]	8.698 (1)
c [Å]	4.731 (1)
V [Å^3]	229.91 (2)
Z	2
T [K]	293
ρ_{calcd} [g cm^{-3}]	2.407
2θ range [°]	7–75
parameters	18
R_p[a]	0.097
R_{wp}[a]	0.121
R_F^2[a]	0.128
χ^2	1.860

[a] See ref. [31] for definitions.

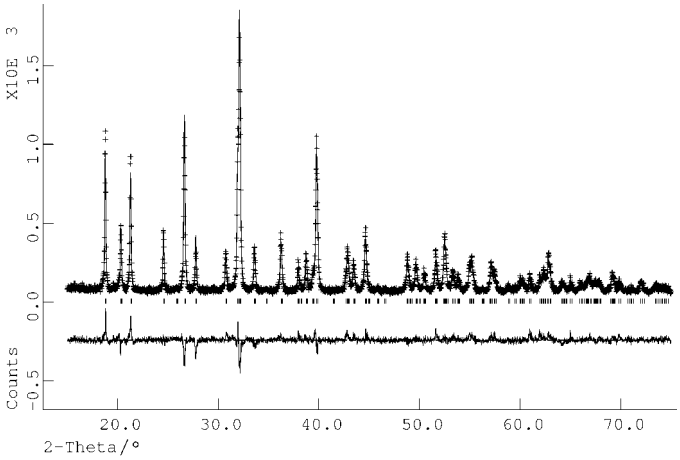

Figure 2. Observed (+ ++) and calculated (——) powder X-ray diffraction profiles for the Rietveld refinement of compound **1**. The bottom curve is the difference plot on the same scale intensity. The tic marks are the calculated 2θ angles for Bragg peaks.

Table 2. Bond lengths [Å] and angles [°] for the nonhydrogen atoms for compound **1**.

O1–Ni	2.10(1)	O2–P	1.45(1)
O2–Ni	2.09(1)	O3–P	1.59(1)
O2′–Ni	2.18(1)	C–P	1.91(1)
O3–Ni	2.10(1)		
O1-Ni-O2	91.3(3)	O3-Ni-O1	168.6(5)
O1-Ni-O2′	89.2(3)	O2-P-O2	106.2(8)
O2-Ni-O2	103.2(4)	O3-P-O2	117.3(5)
O2′-Ni-O2	96.5(3)	C-P-O2	106.8(5)
O3-Ni-O2	95.8(3)	C-P-O3	101.6(8)
O3-Ni-O2′	81.1(4)		

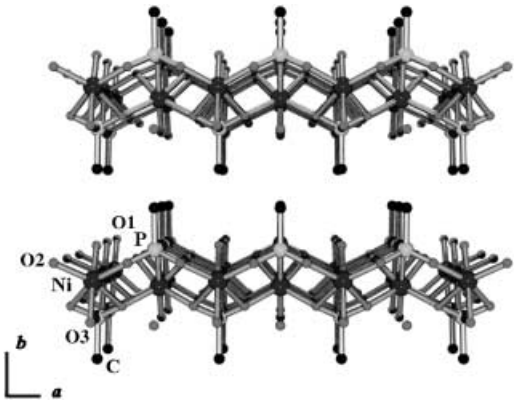

Figure 3. Unit-cell packing of compound **1** viewed along the *c* axis.

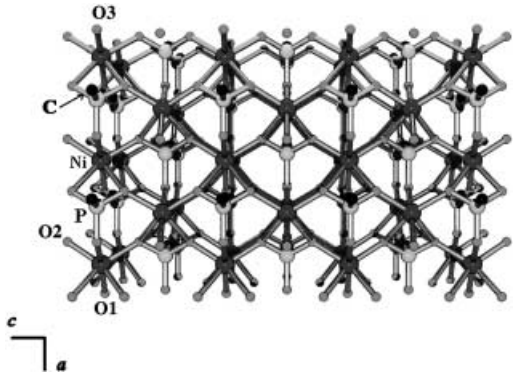

Figure 4. Structure of compound **1** viewed along the *b* axis.

Structural characterisation of $[Ni\{CH_3\text{-}(CH_2)_{17}\text{-}PO_3\}(H_2O)]$ (2): The X-ray powder diffraction spectrum of compound **2** was also recorded and it is shown in Figure 5. The diffraction patterns in the low-angle region are dominated by the (0*k*0) reflections, which were used to estimate the interlayer spacing. The patterns could be indexed assuming the orthorhombic space group $Pmn2_1$ with the following unit-cell parameters: $a = 5.478(7)$, $b = 42.31(4)$, $c = 4.725(3)$ Å.

0947-6539/03/0906-1326 $ 20.00+.50/0 *Chem. Eur. J.* **2003**, *9*, No. 6

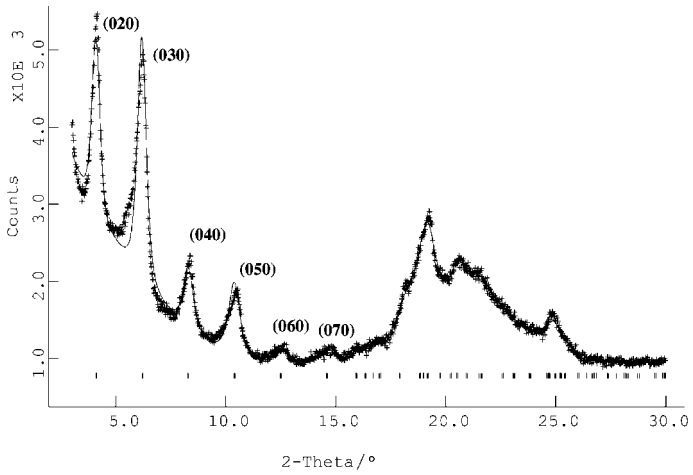

Figure 5. X-ray powder diffraction patterns of compound **2**.

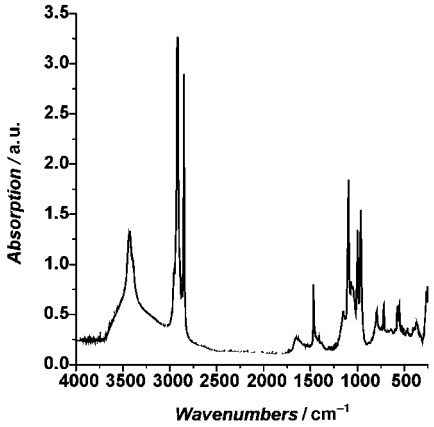

Figure 7. Absorption FTIR spectrum of compound **2** in the KBr region.

The lattice constants *a* and *c* were assumed to be similar to those observed in the Ni^{II} methylphosphonate, demonstrating that the compound is lamellar and originating from self-assembling of bilayers of nickel(II) octadecylphosphonate.

Optical properties: The IR absorption spectrum of compound **1** is reported in Figure 6. It is similar to that of $[Fe(CH_3PO_3)(H_2O)]$[7, 12] and it features two intense bands centred at 3416 cm^{-1} and 3442 cm^{-1}, assignable to an H-O-H stretching

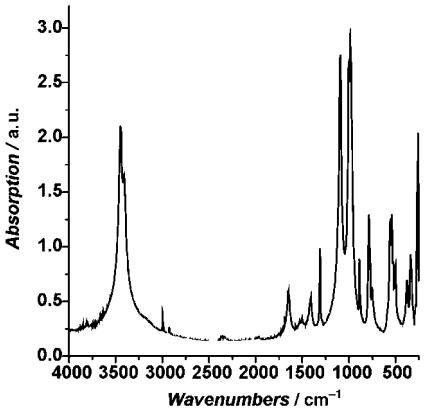

Figure 6. Absorption FTIR spectrum of compound **1** in the KBr region.

vibration of the coordinated water molecule. The strong and sharp nature of these bands confirms that the water is coordinated to the metal ions in these compounds. The medium band, observed at 1648 cm^{-1}, is assigned to the H_2O bending frequency. Three strong bands due to the PO_3^{2-} group symmetric (1000 and 978 cm^{-1}) and asymmetric (1096 cm^{-1}) vibrations are observed in the range 1200–970 cm^{-1}. The complete conversion of the phosphonic acid to its Ni^{II} salt is demonstrated by the absence of an OH stretching vibration of the POH group at ~2700–2550 cm^{-1} and 2350–2100 cm^{-1}.

The IR absorption spectrum of compound **2** is reported in Figure 7 and shows some remarkable differences when compared with that of **1**. Intense peaks were found at 2954, 2916 and 2848 cm^{-1} together with a shoulder at 2870 cm^{-1}; these are assigned to the asymmetric methyl ($\nu_a(CH_3)$: 2954 cm^{-1}), the symmetric methyl ($\nu_s(CH_3)$: 2870 cm^{-1}), the asymmetric methylene ($\nu_a(CH_2)$: 2916 cm^{-1}) and the symmetric methylene ($\nu_s(CH_2)$: 2848 cm^{-1}) stretches of the octadecyl group. It is well known that the position and the shape of the $\nu_a(CH_2)$ and $\nu_s(CH_2)$ absorption bands reflects the conformational order and packing of the aliphatic chains in monolayers.[16] For long-chain hydrocarbons when the aliphatic chain is in all-*trans* conformation the energy of the $\nu_a(CH_2)$ band ranges between 2918–2920 cm^{-1}. The observed position of the $\nu_a(CH_2)$ band at 2918 cm^{-1} implies that alkyl chains are in a fully extended all-*trans* conformation. Another indication of the state of the hydrocarbon chains comes from the $\nu_s(CH_2)$ band. The peak position of this band for crystalline hydrocarbons lies at 2850 cm^{-1} and shifts to a higher value, 2856 cm^{-1}, as the organic chains become less packed. The appearance of the band at 2848 cm^{-1} is consistent with a high density crystalline phase. The presence of two bands at 3430 cm^{-1} and a shoulder at 3396 cm^{-1} and a band at 1660 cm^{-1} in the spectrum indicates that water is coordinated to the metal ion.[17] In the region 900–1800 cm^{-1} of the infrared spectrum, a medium intense peak at 1468 cm^{-1} and a weak one at 1408 cm^{-1} are assigned to the methylene scissor deformation bands. An intense peak at 1150 cm^{-1} and a progression of weak peaks up to 1400 cm^{-1} are assigned to the CH_2 rocking and wagging modes of all-*trans* alkyl chains in this compound (absent in the other one). The band at 1096 cm^{-1} is assigned to the asymmetric PO_3^{-2} stretch and bands between 1066 and 962 cm^{-1} to the symmetric $[PO_3]^{-2}$ stretches; these split as a result of lower than C_{3v} local symmetry of the phosphonate groups (cf. the IR spectrum of compound **1**).

The reflectance spectra in the visible and near-infrared regions of the two compounds display three bands with peaks centred at 7600, 12800 and 23600 cm^{-1}. These bands are characteristic of Ni^{II} in octahedral environment,[18] and correspond to the following electronic transitions: $^3A_{2g} \rightarrow {}^3T_{2g}(F)$, $^3A_{2g} \rightarrow {}^3T_{1g}(F)$, $^3A_{2g} \rightarrow {}^3T_{1g}(P)$.

Magnetic properties of $[Ni(CH_3PO_3)(H_2O)]$ (1): Static magnetic susceptibility measurements were made on a polycrystalline sample with an applied magnetic field of 50 Oe in the temperature range 5 to 250 K, by using a SQUID magne-

  0947-6539/03/0906-1327 $ 20.00+.50/0

tometer. The $1/\chi$ versus T and χT versus T plots are reported in Figure 8. The $1/\chi$ versus T plot is linear above 120 K; this is typical behaviour for a paramagnet. The fit to the data at

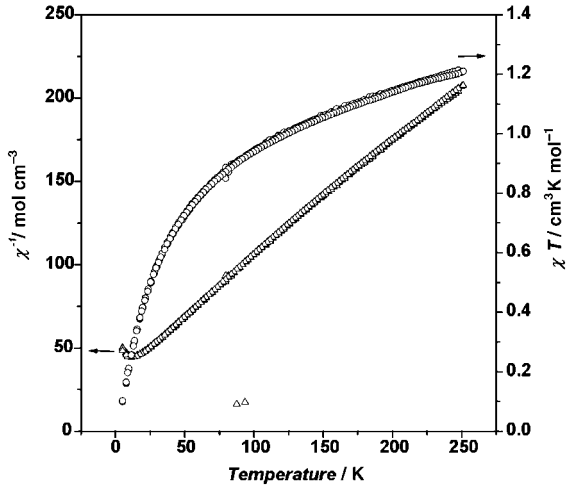

Figure 8. $1/\chi$ versus T plot for compound **1** and χT versus T in the temperature range 20–270 K.

temperatures above 120 K gave values of Curie (C) and Weiss (θ) constants of 1.1578 $cm^3 K mol^{-1}$ and -32 K, respectively. The value of C corresponds to an effective magnetic moment of 3.04 μ_B, a value that is consistent with the presence of a d^8 ($S=1$) electronic configuration, as expected for a Ni^{II} ion.[18] The negative value of the Weiss constant ($\theta=-32$ K) indicates strong antiferromagnetic near-neighbour exchange couplings between the adjacent Ni^{II} ions. Deviation from Curie–Weiss behaviour occurs below 120 K, below which the magnetic susceptibility increases until a broad peak at $\sim$12.0 K is observed. Figure 9 shows the susceptibility versus temperature plot from 5–270 K for this compound. The broad maximum in the temperature-dependent static magnetic susceptibility is characteristic of antiferromagnetic exchange couplings. Based on the fact that the compound has a layered structure, the magnetic behaviour of compound

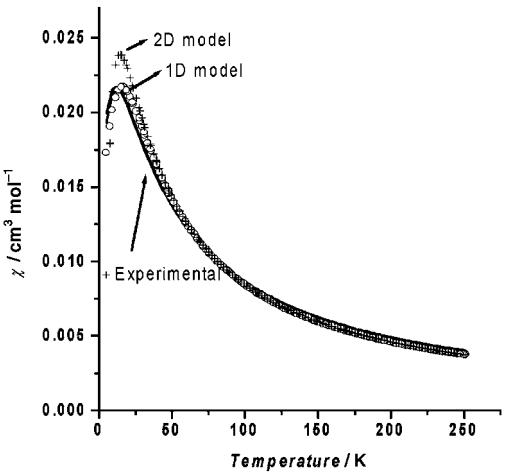

Figure 9. Temperature dependence of χ versus T plot for compound **1** in the temperature range 20–270 K. The 1D and 2D lines are the fit to the 1D and 2D Heisenberg models, respectively (see text).

1 can be analysed in terms of a 2D square-planar Heisenberg model for an $S=1$ system. In this model the position of the maximum in the χ versus T plot is related directly to the intraplanar exchange constant J/k. The relationship between the $T_{(\chi max)}$ and the exchange coupling value J/k, for an S system, is, according to De Jongh and Miedema, given by Equation (1):[19]

$$\tau = kT_{(\chi max)}/|J|S(S+1) \quad (1)$$

For a magnetic $S=1$ system, τ is 2.20 and, therefore, the estimated J/k value is -2.7 K. The fit of the χ versus T plot was also made by using the analytical expression reported by Lines[20] for a 2D square-planar Heisenberg model from a high-temperature expansion series studied by Rushbrooke and Wood [Eq. (2)]:[21]

$$\chi = (2Ng^2\mu_B{}^2/3kT)[1+Ax+Bx^2+Cx^3+Dx^4+Ex^5+Fx^6]^{-1} \quad (2)$$

in which $x=J/kT$ and A, B, C, D, E, F are parameters that depend upon the S value. For $S=1$: $A=5.3333$, $B=9.77778$, $C=9.48148$, $D=19.0617$, $E=45.08971$ and $F=25.46392$.

As a result of the fit reported in Figure 9, it can be concluded that the 2D Heisenberg model does not work in this system. The discrepancy can be explained by the fact that the layer is not really square planar, as assumed in the 2D model, but a corrugated or crenelated one. An attempt has also been made by using a 1D Heisenberg model, but the quality of the fit has not improved. A similar magnetic behaviour has been observed previously in $[Ni(NH_4)(PO_4)(H_2O)]$.[22] This purely inorganic compound is lamellar, it crystallises in the same orthorhombic space group $Pmn2_1$ of compound **1** and it has the same metal–oxygen phosphorus layer, formed by $\{NiO_6\}$ chromophores. The NH_4^+ ions lie in the interlayer region, and the organic part of the phosphonic groups are replaced by the phosphate oxygen. The interlayer distance is similar in value. In the latter the magnetic measurements were carried out down to $T=1.8$ K, but no sign of 3D long-range antiferromagnetic ordering was observed.

Magnetic properties of $[Ni\{CH_3\text{-}(CH_2)_{17}\text{-}PO_3\}(H_2O)]$ (2): Static magnetic susceptibility measurements were performed on a polycrystalline sample of **2** in the applied magnetic field of 200 Oe and in the temperature range of 5–270 K, both in zero and field-cooled modes. The temperature dependence of the molar magnetic susceptibility plotted as $1/\chi$ versus T is reported in Figure 10. The plot is linear and it obeys to the Curie–Weiss law. The deduced C value, that is, 1.25 $cm^3 K mol^{-1}$, is in agreement with the expected value for Ni^{II} d^8 ($S=1$) electronic configuration. The Weiss constant is negative in value: $\theta=-24$ K. The χT versus T plot decreases slowly on lowering the temperature down to 30 K and then starts to rise again. Below this temperature the magnetic behaviour of **2** is different from that observed in **1**. Zero-field (zfc) and field-cooled (fc) M versus T plots under an applied field of 10 Oe were measured and are reported in Figure 11. The two plots do not overlap below $T=21$ K and the bifurcation point is at $T\sim21$ K. The zfc magnetisation

0947-6539/03/0906-1328 $ 20.00+.50/0 *Chem. Eur. J.* **2003**, *9*, No. 6

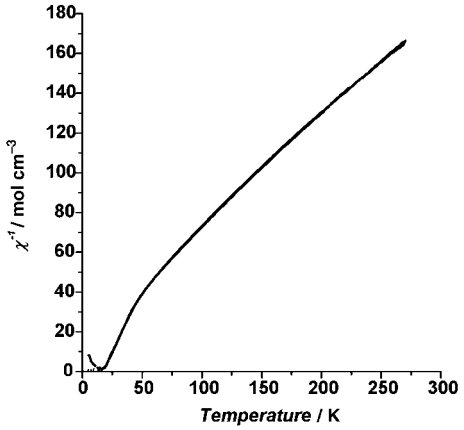

Figure 10. Temperature dependence of $1/\chi$ versus T plot of compound **2** in the temperature range 20–270 K.

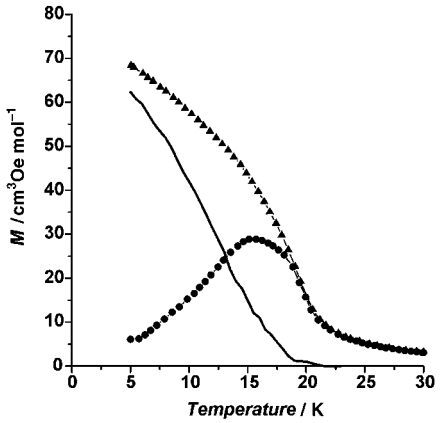

Figure 11. Temperature dependence of M versus T plot for compound **2** in the temperature range 5–30 K in zero-field (●) and field cooling modes (▲). Irreversible magnetisation, ΔM_{fc-zfc} as obtained from the difference of the fc and zfc plots (——).

increases up to ~16 K reaching a broad maximum and then decreases again slowly down to 5 K. The fc magnetisation shows a continuous increase on lowering the temperature. The experiment provides an indication that the compound is magnetically ordered below $T = 21$ K. The difference between the fc and zfc magnetisations depicted in Figure 11 represents the irreversible magnetisation (ΔM_{fc-zfc}). The value of ΔM_{fc-zfc} starts to increase on lowering the temperature and it reaches 60 $cm^3\,Oe\,mol^{-1}$ at $T \sim 5$ K. The temperature at the onset of the zfc plot is taken as the critical temperature T_N. Hysteresis loops were observed at different temperatures below $T \leq 20$ K for applied magnetic fields <1 Tesla. The plot recorded at $T = 5$ K is reported in Figure 12 and is not characteristic of a ferromagnetically ordered material. In fact, at 3 T, the magnetisation does not saturate and the value at that field is 18% in value of that expected for the fully aligned moment Ni^{2+} (i.e., 11170 $cm^3\,Oe\,mol^{-1}$). This behaviour is typical of a weak ferromagnet. The presence of the weakly ferromagnetic state is due to the "spin-canting".[13] The local spins in this ordered state are not perfectly antiparallel, leading to a net spontaneous magnetisation that saturates in a small field.

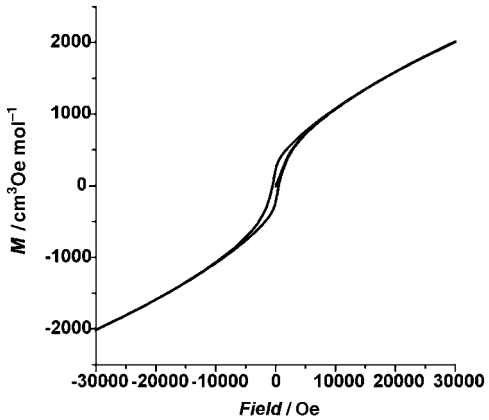

Figure 12. Hysteresis loop of $Ni[CH_3\text{-}(CH_2)_{17}\text{-}PO_3(H_2O)]$ measured at $T = 5$ K.

The value of magnetisation increases nonlinearly up to 3.0 T, the highest measured field. From the plot the values of the remnant magnetisation (M_{remn}) and of the coercive field (H_c) can be directly obtained; they are 220 $cm^3\,Oe\,mol^{-1}$ and 516 Oe, respectively. The estimation of the value of M_s (5 K) from Equation (3) is difficult:

$$M(H,T) = M_s(T) + \chi(T)\,H \quad (3)$$

If we approximate the value of M_s to the M_{remn} found at 5 K, then the canting angle is estimated to be $\sim 1^\circ$.

Conclusion

Two Ni^{II} alkylphosphonates have been synthesised by reaction of $NiCl_2 \cdot 6H_2O$ and the relevant phosphonic acid in water in presence of urea. The reaction affords pure and microcrystalline yellow-green solids. The compound $[Ni(CH_3PO_3)(H_2O)]$ (**1**) has a layered structure, with the inorganic and organic layers alternating along the b axis of the unit cell. The inorganic sheet is made of Ni^{II} ions, octahedrally coordinated by five phosphonate oxygen atoms and one oxygen atom from a water molecule. The octahedron is distorted due to the fact that two oxygen atoms of the phosphonate ligand bond to two Ni atoms and one acts as monodentate. The antiferromagnetic behaviour observed in **1** cannot be rationalised in terms of 2D or 3D Heisenberg models. The compound $[Ni\{CH_3\text{-}(CH_2)_{17}\text{-}PO_3\}(H_2O)]$ (**2**) was prepared for the first time and characterised by X-ray diffraction and IR spectroscopy; it has a layered structure. The position and the shape of the $\nu_a(CH_2)$ and $\nu_s(CH_2)$ absorption bands reflect the conformational order and packing of the aliphatic chains in monolayers.[16] The observed position of the $\nu_a(CH_2)$ band at 2918 cm^{-1} implies that alkyl chains are in a fully extended all-*trans* conformation. The presence of the split bands in the $-PO_3^{2-}$ stretching mode range, that is, at 1100–950 cm^{-1}, indicates that the local symmetry around P atom is lower than C_{3v}. The structure of the Ni^{II} octadecylphosphonate compound is lamellar and the interlayer distance is 42.31 Å, a distance which is lower than that observed in films of bilayers of Mn^{II}

  0947-6539/03/0906-1329 $ 20.00+.50/0

octadecylphosphonates (i.e., 48.5 Å) obtained by Langmuir–Blodgett techniques.[23] Surprisingly, the magnetic properties of Ni^{II} octadecylphosphonate at low temperatures are different to those shown by **1**; its behaviour is typical of a weak-ferromagnet. The broad maximum in the χ versus T plot consistent with a low-dimensional magnetic system is absent. An estimation of the intraplanar super-exchange J/k value is thus prevented. The hysteresis loop observed at $T \sim 20$ K, a temperature that corresponds to the bifurcation of the M versus T plot, indicates that the solid is still magnetised, and that the transition to 3D long-range antiferromagnetic ordering is at $T \sim 21$ K. The presence of the weakly ferromagnetic state is due to the "spin-canting".[13] The local spins in this ordered state are not perfectly antiparallel; this leads to a net spontaneous magnetisation that saturates in a small field.

On the basis of the similarity of the lattice in both the reported compounds, it is difficult to understand why at low temperatures the magnetic behaviour of compound **2** is different from that of **1**; it is also difficult to suggest which mechanism is responsible for the spin-canting: that is, single-ion magnetic anisotropy,[13, 24] and/or the so-called antisymmetric Dzyaloshinsky–Moriya (DM) exchange coupling.[25, 26]

Experimental Section

Materials and methods: Methylphosphonic acid ($CH_3PO_3H_2$) was of analytical grade (Aldrich) and was used without further purification. Urea was of analytical grade (Carlo ERBA). The octadecylphosphonic acid CH_3-$(CH_2)_{17}$-PO_3H_2 was prepared according to literature methods and the purity checked by elemental analysis.[27] HPLC water was used as solvent.

Synthesis of [Ni(CH_3PO_3)(H_2O)] (1): This compound was recently prepared by neat reaction between Ni^{II} hydroxide and methylphosphonic acid at the melting point of the acid.[15] We have prepared Ni^{II} organophosphonates from solution. For this purpose $NiCl_2 \cdot 6H_2O$ (2.33 g, 9.8 mmol) was dissolved in water (35 mL). The solution was filtered and added to a clean aqueous solution containing methylphosphonic acid (0.94 g, 9.8 mmol) and urea (1.17 g, 19.5 mmol). The resulting solution was refluxed for 3 days at 80 °C, then the temperature was raised up to 90 °C and reflux was continued for other six days. A greenish-yellow microcrystalline solid was separated. The product was washed several times with water, then methanol and finally dried to the air. Elemental analysis calcd (%) for $NiCH_5O_4P$: C 7.03, H 2.95, H_2O 10.54; found: C 7.02, H 2.92, H_2O 10.41. This compound was also prepared by a hydrothermal method and similar elemental analysis results were obtained.

Synthesis of [Ni{CH_3-$(CH_2)_{17}$-PO_3}(H_2O)] (2): The compound was prepared by following the above-described procedure. $NiCl_2 \cdot 6H_2O$ (1.0 g, 4.2 mmol) was dissolved in water (30 mL). The solution was filtered and added to a clean aqueous solution containing octadecylphosphonic acid (1.00 g, 3 mmol) and urea (0.37 g, 6 mmol). The resulting solution was refluxed for a week at 80 °C. A greenish-yellow microcrystalline solid was separated. The compound was then washed three times with water and then with hot methanol, and finally dried to the air. Elemental analysis calcd (%) for $NiC_{18}H_{39}O_4P$: C 52.84, H 9.11, H_2O 4.40; found: C 53.44, H 9.87, H_2O 4.29.

Characterisation and physical measurements: Elemental analyses were performed by the Servizio di Microanalisi della Area di Ricerca di Roma del CNR. Thermogravimetric (TGA) data were obtained in flowing dry nitrogen at a heating rate of 10° min^{-1} on a Stanton-Redcroft STA-781 thermoanalyser. The FT-IR absorption spectra were recorded on a Perkin–Elmer 621 spectrophotometer by using KBr pellets. Static magnetic susceptibility measurements were performed by using a Quantum Design MPMS5 SQUID magnetometer in fields up to 5 T. A cellulose capsule was filled with a freshly prepared polycrystalline sample and placed inside a polyethylene straw at the end of the sample rod. All the experimental data were corrected for the core magnetisation using Pascal's constants.

X-ray data collection: Room temperature X-ray powder diffraction data were recorded on a Seifert XRD-3000 diffractometer, Bragg–Brentano geometry, equipped with a curved graphite monochromator ($\lambda(Cu_{K\alpha 1,2}) =$ 1.54056/1.5444 Å) and a scintillation detector. The data were collected with a step size of 0.02°, $\Delta 2\theta$ and at count time of 8 s per step of 0.2° min^{-1} over the range $4° < 2\theta < 80°$. The sample was mounted on a flat glass plate giving rise to a strong preferred orientation. The diffractometer zero point was determined from an external Si standard.

Structure solution and refinements of [Ni(CH_3PO_3)(H_2O)] (1): The low-angle powder diffraction patterns of the compound **1** were indexed by using the TREOR program,[28] which suggested a primitive orthorhombic cell with the following unit-cell parameters: $a = 5.59(1)$, $b = 8.70(1)$, $c =$ 4.74(1) Å. The fit was characterised by the figure of merit $M'(20) = 124$ and $F(20) = 33$ (0.0165, 46). The unit-cell parameters and the space group were found to be the same as those reported for [Ni(CH_3PO_3)(H_2O)] prepared by Hix et al.;[15] this shows that the same nickel compound can be obtained by two different synthetic procedures. The systematic absences observed in the XRD spectrum of [Ni(CH_3PO_3)(H_2O)] were consistent with the space group $Pmn2_1$ and later confirmed by successful solution and Rietveld refinement. The starting atomic coordinates were found by using the EXPO[29] program, which afforded the location of the Ni, P, C and O atoms. The asymmetric unit was build up by the help of the program PowderCell.[30] The structure was refined with the Rietveld method by using a PC version of the crystal structure analysis package program GSAS[31a] with the graphical user interface EXPGUI.[31b] Powder diffraction patterns were calculated for this model in the orthorhombic space group $Pmn2_1$, and by using the unit-cell parameters refined by a least-squares procedure described above. Data were evaluated in the 7–75° 2θ angular range. By using the utility CONVX,[32] the raw data were transferred to the GSAS program package[31a] for full profile refinement. Initially the scale factor, the lattice parameters, the background coefficients and the peak shape were refined by the Le Bail method.[33] Atomic positions were refined and soft constraints for the ligand were introduced by fixing the P–C and P–O bonds at ~1.80 Å and ~1.50 Å, respectively; otherwise the refinement produces incorrect P–C and P–O bond lengths. In the last stage of the process the atomic isotropic thermal parameters were also refined. A correction was made for the preferred orientation [010], as also suggested by the EXPO analysis of the data by using the March–Dollase method in the GSAS suite of programs.

Acknowledgement

This work is supported by the Consiglio Nazionale delle Ricerche (Italy) and the Academy of Scientific Research and Technology (Egypt) in the framework of their bilateral collaboration agreement. C.B. also thanks F. Federici for the synthesis of the compounds.

[1] G. Alberti in *Comprehensive Supramolecular Chemistry*, *Vol. 7* (Eds.: J. L. Atwood, J. E. D. Davies, D. D. MacNicol, F. Vögtle), Pergamon, Oxford, **1996**, pp. 151–185 and references therein.
[2] D. M. Poojary, B. Zhang, A. Clearfield, *J. Am. Chem. Soc*. **1997**, *119*, 12550–12559.
[3] A. Clearfield, *Prog. Inorg. Chem*. **1998**, *47*, 371–510.
[4] G. Cao, H. Hong, T. E. Mallouk, *Acc. Chem. Res.* **1992**, *25*, 420–427.
[5] G. Cao, H. Lee, V. M. Lynch, L. M. Yacullo, *Chem. Mater*. **1993**, *5*, 1000–1006
[6] a) G. Cao, H.Lee, V. M. Lynch, T. E. Mallouk, *Inorg. Chem*. **1988**, *27*, 2781–2785; b) Y. Zhang, K. J. Scott, A. Clearfield, *Chem. Mater*. **1993**, *5*, 495–499.
[7] C. Bellitto, F. Federici, M. Colapietro, G. Portalone, D. Caschera, *Inorg. Chem*. **2002**, *41*, 709–714.
[8] C. Bellitto in *Magnetism: Molecules to Materials*, *Vol. 2* (Eds.: J. S. Miller, M. Drillon), Wiley-VCH, Weinheim, **2001**, pp. 425–456.
[9] a) C. Bellitto, F. Federici, S. A. Ibrahim, *Chem. Commun*. **1996**, 759–760; b) C. Bellitto, F. Federici, S. A. Ibrahim, *Chem. Mater.* **1998**, *10*, 1076–1082.

  0947-6539/03/0906-1330 $ 20.00+.50/0 *Chem. Eur. J.* **2003**, *9*, No. 6

[10] C. Bellitto, F. Federici, S. A. Ibrahim, M. R. Mahmoud, *Mater. Res. Soc. Symp. Proc.* **1999**, *547*, 487–492.
[11] C. Bellitto, F. Federici, A. Altomare, R. R. Rizzi, S. A. Ibrahim, *Inorg. Chem*. **2000**, *39*, 1803–1808.
[12] A. Altomare, C. Bellitto, S. A. Ibrahim, M. R. Mahmoud, R. R. Rizzi, *J. Chem. Soc. Dalton Trans.* **2000**, 3913–3919.
[13] See, for example: R. L. Carlin, *Magnetochemistry*, Springer, Berlin, **1986**, pp. 149–152.
[14] Q. Gao, N. Guillou, M. Nogues, A. K. Cheetham, G. Ferey, *Chem. Mater*. **1999**, *11*, 2937–2947.
[15] C. B. Hix, K. D. M. Harris, *J. Mater. Chem*. **1998**, *8*, 579–584.
[16] M. D. Porter, T. B. Bright, D. L. Allara, C. E. D. Chidsey, *J. Am. Chem. Soc*. **1987**, *109*, 3559–3568.
[17] K. Nakamoto, *Infrared and Raman Spectra of Inorganic and Coordination Compounds*, 3rd ed., Wiley, New York **1978**.
[18] B. N. Figgis, *Introduction to Ligand Fields*, Interscience, London **1966**, pp. 220–222.
[19] J. DeJongh, A. R. Miedema, *Adv. Phys.* **1974**, *23*, 1.
[20] M. E. Lines, *J. Phys. Chem. Solids* **1970**, *31*, 101–116.
[21] G. S. Rushbrooke, P. J. Wood, *Mol. Phys.* **1958**, *1*, 257–285.
[22] A. Goni, J. L. Pizarro, L. M. Lezama, G. E. Barberis, M. I. Arriortua, T. Rojo, *J. Mater. Chem*. **1996**, *6*, 421–427.
[23] C. T. Seip, G. E. Granroth, M. W. Meisel, D. R. Talham, *J. Am. Chem. Soc.* **1997**, *119*, 7084–7094.
[24] T. Moriya, *Phys. Rev.* **1960**, *120*, 91–98.
[25] T. Moriya, *Phys. Rev.* **1960**, *117*, 635–647.
[26] I. Dzyaloshinsky, *J. Phys. Chem. Solids* **1958**, *4*, 241–255.
[27] See, for example: *Structure and Mechanism of Organophosphorus Chemistry*, Academic Press, New York, **1965**.
[28] a) P. E. Werner, L. Eriksson, M. Westdahl, *J. Appl. Crystallogr*. **1985**, *18*, 367–370; b) A. Altomare, C. Giacovazzo, A. Gagliardi, A. A. G. Moliterni, R. Rizzi, P. E. Werner, *J. Appl. Crystallogr*. **2000**, *33*, 1180–1186.
[29] A. Altomare, M. C. Burla, G. Cascarano, C. Giacovazzo, A. Gagliardi, A. G. Moliterni, G. Polidori, *J. Appl. Crystallogr*. **1999**, *32*, 339–340.
[30] G. Noltze, W. Kraus, http://www.ccp14.ac.uk/ccp/webmirrors/powdcell/a_v/v_1/powder/e-cell.html
[31] a) A. C. Larson, R. B. Von Dreele, GSAS: Generalized Structure Analysis System: Report LAUR 86–748, Los Alamos National Laboratory: Los Alamos NM **1994**; b) "EXPGUI a graphical user interface for GSAS": B. H. Toby, *J. Appl. Crystallogr*. **2001**, *34*, 210–213.
[32] For the program utility CONVX by M. E. Bowden, see web page in ref. [30].
[33] A. Le-Bail, H. Duroy, J. L. Fourquet, *Mater. Res. Bull*. **1988**, *23*, 447–452.

Received: July 23, 2002 [F4277]

  0947-6539/03/0906-1331 $ 20.00+.50/0